Semiconductor Physics, Quantum Electronics & Optoelectronics, 2024. V. 27, No 4. P. 489-494.

Sensors

Magnetic field induced anomalous shift of plasmon resonance peak in Al-based plasmon-polariton photodetectors

R.A. Redko[1,2], S.V. Mamykin[1], O.S. Kondratenko[1], Ye.M. Savchuk[1]

[1]V. Lashkaryov Institute of Semiconductor Physics, NAS of Ukraine
[2]State University of Information and Communication Technologies
Corresponding author e-mail: redko.rom@gmail.com

Abstract. The influence of magnetic field on Ψ(λ) and Δ(λ) dependences of Al-based plasmon-polariton photodetectors (PPPD) at different magnetic flux densities (100 and 300 mT) and magnetic field directions was investigated. It was obtained that the action of the magnetic field results in the shift of the surface plasmon resonance peak (SPR) position and a change in its intensity. Particularly, in the configuration $\vec{B} \perp \vec{n}$ ($\vec{B}$ and $\vec{E}$ are collinear) the noted effects were the most pronounced. Additionally, it was found that the magnetic-induced effects are sensitive to the angle of incidence, particularly they enhance with decreasing the angle of incidence. Therefore, they were the most pronounced at the smallest angle in our experiment (20°). The possible physical mechanisms of observed phenomena are discussed. The obtained results can open up new opportunities in the design of optoelectronic sensors of the magnetic field or high-speed optical modulators.

Keywords: surface plasmon resonance, magnetic field, plasmon-polariton photodetector.

https://doi.org/10.15407/spqeo27.04.489
PACS 42.79.Pw, 71.36.+c, 73.20.Mf, 85.60.Gz

Manuscript received 25.09.24; revised version received 16.10.24; accepted for publication 13.11.24; published online 06.12.24.

1. Introduction

Surface plasmon resonance (SPR) is a powerful method of the real-time measuring of interactions with ultra-high sensitivity. The SPR has gained great popularity and represents a viable choice for many applications, from life sciences to pharmaceutics, agrifood, and environmental monitoring of harmful substances [1]. Fundamental phenomena occurring at SPR detection are well-known and used to produce various high-quality sensor systems. However, there are several features that take place when SPR is observed at the applied external magnetic field. Namely, the shift of the SPR peak position in the transmittance (reflectance) spectrum is caused by the action of a magnetic field on the motion of electrons by the Lorentz force. This phenomenon differs from the Faraday effect, which is a magneto-optical phenomenon when the polarization direction of linearly polarized light is rotated when passing through a transparent material with the magnetic field applied along the direction of light propagation [2].

The semiconductor plasmon-polariton photodetectors (PPPD) proposed in [3] are structures with a built-in near-surface potential barrier. It can be a shallow *p-n* junction or the Schottky barrier with a metal front contact (usually Au or Ag) periodically profiled in a diffraction grating (DG). This micro-relief allows the excitation of SPR due to the matching of the wave vector of the surface plasmon polariton wave and light. The near-surface potential barrier in the PPPD produces a photovoltage/photo-current between the gold barrier contact and the ohmic contact formed on the opposite side of the semiconductor wafer. The photocurrent has a resonant nature. It has a maximum only at a certain polarization, wavelength, and angle of light incidence when the SPR is excited. Since the SPR is a surface wave, it is very sensitive to the state of the surface as well as to the magnetic field induced changes in the optical properties of metal film.

Up to now, there are several high-quality and ultra-highly sensitive sensors [1, 4–6] based on the SPR system. However, all of them require an additional magnetic-sensitive substance – magnetic fluid, which is sensitive to an external magnetic field and plays the role of the external environment that besides the main metal material, defines the SPR-peak position. Any changes in the magnetic properties of this fluid result in changes in the SPR signal. However, magnetic fluid needs to be prepared in special conditions, besides storage, operation, and movement require special conditions. Based on our

previous experience in SPR-related sensor systems [7–9] and works aimed at magnetic field induced effects [10–14], we argue that the SPR signal can be sensible for the magnetic field action without any additional magnetic fluid. This statement is based on the nature of SPR related to electron oscillations under electromagnetic field action and the well-known Lorenz force that appears in magnetic fields and rotates electrons with a cyclotron frequency. This rotation will result in a change in the SPR-related peak position. Investigations in this field are limited and carried out with ferromagnetic substrates [14, 15] or have theoretical character [16–19].

Therefore, this work aims to investigate the influence of the magnetic field on the SPR characteristics of Al-based plasmon-polariton photodetectors.

2. Experimental

2.1. Sample preparation

For the fabrication of PPPDs, a pre-made *p*-*n* junction on *n*-Si (111) with a burial depth of 100 nm and formed Ohmic rear contacts with Ti/Ni 25/250 nm were used. The necessary periodic relief structures (gratings) on the silicon surface were created using the method of interference lithography using the chalcogenide photoresist thermally deposited in vacuum [3]. A particular feature of this technology, compared to the standard one where the grating is etched on the semiconductor, is the profiling exclusively of the metallic plasmon-carrying Al film. This maintains a flat metal/semiconductor interface with a weak recombination of photo-generated carriers. Such PPPD has a simpler construction and good resonant properties [3].

The procedure of Al gratings fabrication on the Si surface is briefly described as follows [20]. Before installation into the vacuum chamber, the working side of the Si wafer was cleaned in ethyl alcohol and a 5% aqueous solution of HF, followed by rinsing with distilled water and drying with compressed air. The subsequent steps involved sequential vacuum thermal deposition of an adhesive Cr layer with a mass thickness of ~ 3 nm and an Al layer of optimal thickness onto the Si surface. This thickness will determine the depth of modulation of the surface relief, *D*. After cooling the wafer to room temperature, a layer of photoresist $As_{40}S_{40}Se_{20}$ with a thickness of ~150 nm was deposited on the Al surface. The photoresist was exposed in the interference zone of two coherent laser beams emitted by a helium-cadmium laser (wavelength λ = 441.6 nm). The spatial period of the light intensity distribution in the interference zone depended on the convergence angle of the beams and determined the grating period, *a*. After exposure, selective etching of the photoresist was performed to form a mask that allows the etchant access to the open areas of the Al layer.

The etchant used for the photoresist $As_{40}S_{40}Se_{20}$ contained ethylenediamine ($C_2H_8N_2$) as an active substance and dimethyl sulfoxide (C_2H_6OS) as a solvent, in a ratio of ~ 1:9. At the optimal etchant temperature (20…25 °C), the etching process took close to 3 minutes.

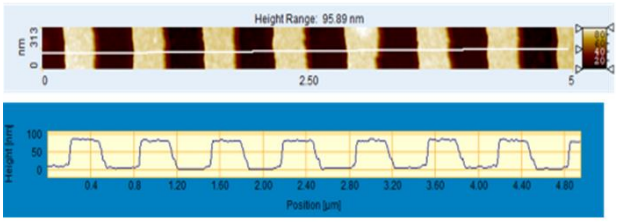

Fig. 1. AFM image of the frontal surface (a) and cross-section (b) of the grating with optimal geometric parameters.

After creating the relief lithographic mask, the Al layer in the mask openings was removed using an etchant based on orthophosphoric (H_3PO_4), acetic (H_3COOH) acids, and distilled water in a ratio of 6:2:2. The final steps of forming the relief structure of the PPPD involved removing the lithographic mask and vacuum thermal deposition of an additional Al layer of thickness *d* onto the obtained relief. The aluminum grating (Fig. 1) on the silicon wafer surface provides the excitation of the SPR signal and serves as the upper electrical contact.

The photocurrent of prepared PPPD exhibits resonant properties. Fig. 2 shows the spectral dependences of the photocurrent under polarized light measured at *p*- (curves *1*–*5*) and *s*- (*6*, *7*) light polarization, at various angles of light incidence, as indicated in the figure.

2.2. Ellipsometry measurements

The optical properties of DGs were studied by spectroscopic ellipsometry (SE). The ellipsometry characterization of the samples was performed using a SE-2000 (SEMILAB) multi-angle spectroscopic ellipsometer, which spans the NIR−VIS−UV range (190…2000 nm) with a resolution of 1 nm. The diameter of the focused beam was about 0.4 mm on the sample surface. The

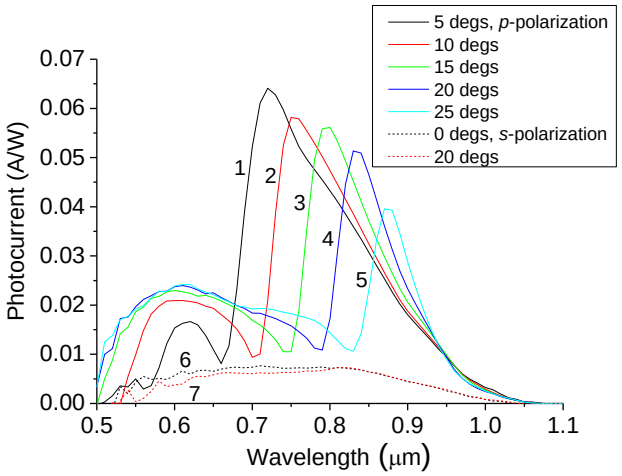

Fig. 2. Spectral dependences of the photocurrent of Al-based PPFD under polarized light, at various angles of incidence and polarization, as indicated in the figure. For interpretation of the colors in the figure(s), the reader is referred to the web version of this article.

experimental ellipsometry angles (Ψ, Δ) are defined by the complex reflectance ratio $\rho = r_p / r_s = \tan\psi e^{i\Delta}$, where r_p and r_s are the complex Fresnel reflection coefficients for *p*- and *s*-polarized light, respectively. tan ψ represents the amplitude ratio of the *p*- and *s*-components of reflected light and Δ describes the phase difference between *p*- and *s*-polarized light.

Since the SPR is observed when measurements are taken perpendicular to the grating lines, the measurements were carried out across the grating lines within the incident angle range 70°…20°. The samples were studied in two different configurations. In the first configuration, the sample was placed directly on the magnet. In the second configuration, the sample was positioned between the magnets and measured in a magnetic field (positions I and II of sample placement). In the absence of a magnetic field, the experimental spectra return to their initial positions.

2.3. Magnetic field action setup

There were several configurations of applied magnetic fields (Fig. 3). These configurations were used at two different magnetic flux densities: 100 and 300 mT. All experiments were provided at room temperature. At the first position, the magnetic field was parallel (antiparallel) to the normal of the sample surface and to the incident beam plane, while at the second one, it was perpendicular to this normal and simultaneously perpendicular to the incident beam plane. At the third position, the magnetic field was perpendicular to the normal of the sample surface and simultaneously parallel to the incident beam plane.

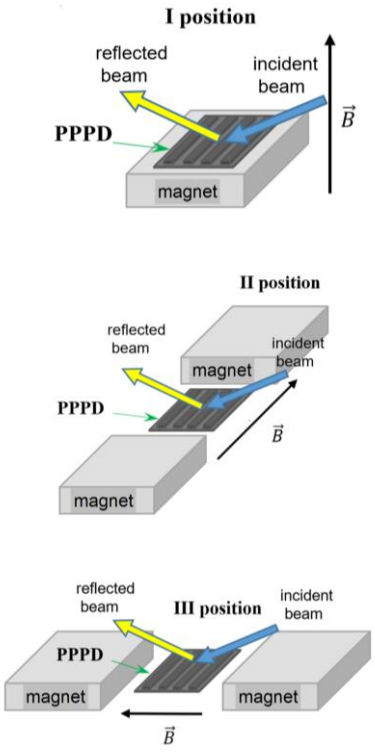

Fig. 3. Three configurations of the experimental setup.

3. Results and discussion

For the first setup position of experimental configuration at $\vec{B} \uparrow\uparrow \vec{n}; \vec{B} \uparrow\downarrow \vec{n}$, and $B = 100$ mT within the angle range 20°…70°, any changes in spectral dependences were very small and did not exceed the measurement error. So, these results are not presented here. While at the same configuration but for a magnetic flux density of 300 mT weak MF (magnetic field)-induced features were detected (Fig. 4). The selected areas from Fig. 4 are presented in Fig. 5 at a magnified scale. All further presented data concern the magnetic flux density of 300 mT.

One can see a weak but detectable blue shift (3-4 nm) of several peaks, induced by the magnetic field. These peaks are located within the 700…1000 nm spectral range. For peaks detected close to 500 nm, no shifts were observed.

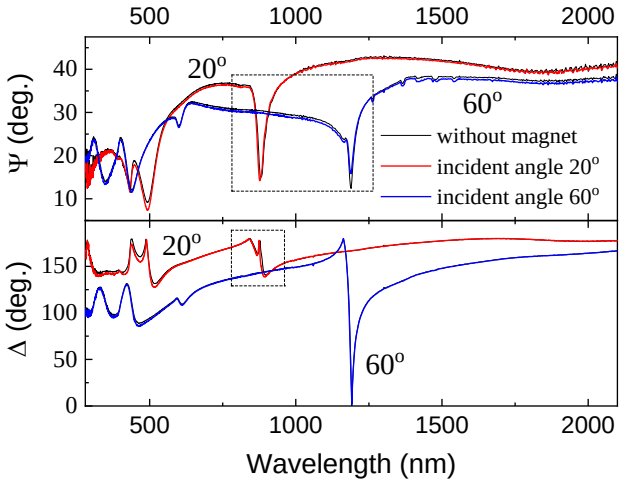

Fig. 4. Experimental Ψ and Δ *vs* wavelength dependences obtained at I position for the incident angle of 20° and 60°.

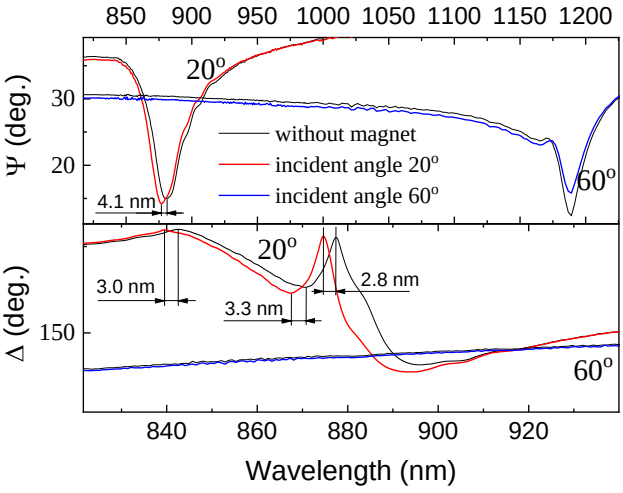

Fig. 5. The magnified scale for the selected areas from Fig. 2.

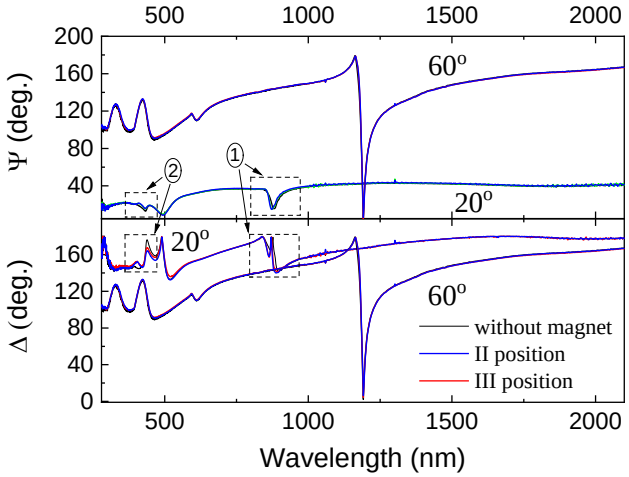

Fig. 6. Experimental Ψ and Δ *vs* wavelength dependences obtained at II and III positions for the incident angle of 20° and 60°.

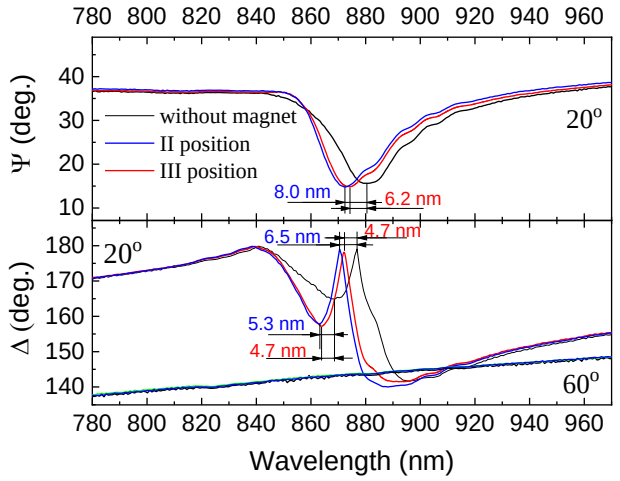

Fig. 7. The magnified scale for the first selected areas from Fig. 6.

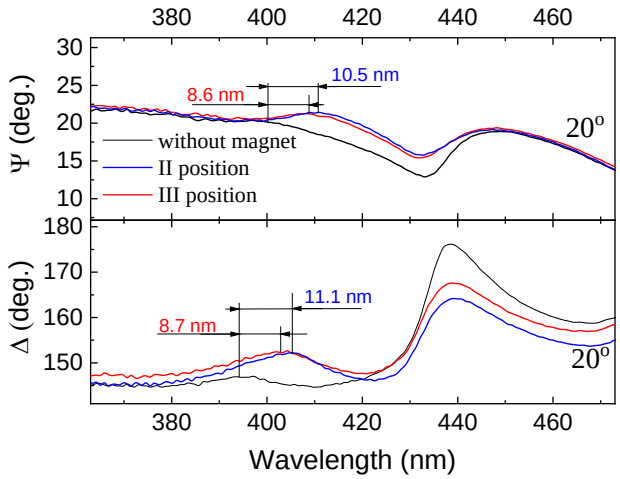

Fig. 8. The second selected areas from Fig. 6 at increased scale.

For the second and third setup positions of experimental configuration, the effect was more pronounced. It was ascertained that magnetic field action results in both blue shift and unsubstantial increase in the amplitude of characteristic SPR peaks in the dependences of studied structures (Fig. 6). It should be noted that there are two spectral ranges where the MF-induced features were observed. The first is within 700…1000 nm (as well as at configuration I), and the second is close to 500 nm.

Fig. 7 shows the spectral range selected by the first rectangle from Fig. 6, at a magnified scale. One can see that at both configurations II and III, the following MF-induced sifts are observed: 4…6 nm for position II and 5…8 nm for position III. These shifts are approximately two times larger than those obtained at position I (Fig. 5).

The largest spectral shift (up to 8 nm) induced by the magnetic field is observed in our experiments at position II (Fig. 7). It is equal to the energy shift of 13 meV for the observed blue shift of the plasmon-polariton wave from 880 to 872 nm at position II of the magnetic field. For III and I positions, these values are equal to 9.7 meV (from 880 to 874 nm) and 4.8 meV (from 880 to 876 nm), respectively. Calculating the energy transferred to a sample in a magnetic field using a well-known formula:

$$E = \mu_B B\,, \qquad (1)$$

where μ_B is Bohr's magneton, B – magnetic flux density, we obtain ~17 μeV at 300 mT. It is three orders of magnitude less than the experimentally observed shift. This peculiarity is unclear and still under discussion.

Besides the blue shifts within the plasmon resonance spectral range, the red shifts also were detected. Fig. 8 demonstrates the second selected areas from Fig. 6. One can see that in this case the shift value is close to 10…11 nm, which is even larger than discussed above. The opposite influence of the same magnetic field on peaks in different spectral ranges is unexpected. But we tend to explain these phenomena within the concept of the optical Hall effect [21]. The observed peculiarities are complex and require further investigation.

4. Conclusions

In summary, the ellipsometry dependences of Ψ and Δ of Al-based PPPD at the applied magnetic field in different configurations have been investigated within the spectral range 190…2000 nm at incident angles of 20°…70°. It was ascertained that the magnetic field leads to both blue and red shifts of the observed peaks and an increase of their amplitude within a certain spectral range. The results and conclusions of this study can be summarized as follows. (i) The MF-induced effects were detected in the non-magnetic composition of PPPD. (ii) The observed peculiarities disappear when the magnetic field action is removed. (iii) The most significant effect of the magnetic field action on the spectral maxima position is observed at the incident angle of 20°. (iv) At sample position II, the MF-induced effect is stronger than in positions I and III.

Acknowledgments

This work was sponsored by the IEEE program "Magnetism for Ukraine 2023", supported by the IEEE Magnetic Society under the Science and Technology Center in Ukraine (STCU) framework.

References

1. Capelli D. Scognamiglio V., Montanari R. Surface plasmon resonance technology: Recent advances, applications and experimental cases. *Trends Anal. Chem.* 2023. **163**. P. 117079. https://doi.org/10.1016/j.trac.2023.117079.
2. Carothers K.J., Norwood R.A., Pyun J. High verdet constant materials for magneto-optical faraday rotation: A review. *Chem. Mater.* 2022. **34**, No 6. P. 2531–2544. https://doi.org/10.1021/acs.chemmater.2c00158.
3. Korovin A.V., Dmitruk N.L., Mamykin S.V. *et al*. Enhanced dielectric environment sensitivity of surface plasmon-polariton in the surface-barrier heterostructures based on corrugated thin metal films with quasi-anticorrelated interfaces. *Nanoscale Res. Lett.* 2017. **12**, No 1. P. 213. https://doi.org/10.1186/s11671-017-1974-3.
4. Huang H., Zhang Z., Yu Y. *et al*. A highly magnetic field sensitive photonic crystal fiber based on surface plasmon resonance. *Sensors*. 2020. **20**, No 18. P. 5193. https://doi.org/10.3390/s20185193.
5. Wang D., Yi Z., Ma G. *et al*. Two-channel photonic crystal fiber based on surface plasmon resonance for magnetic field and temperature dual-parameter sensing. *Phys. Chem. Chem. Phys.* 2022. **24**, No 35. P. 21233–21241. https://doi.org/10.1039/D2CP02778J.
6. Wang D., Zhu W., Yi Z. *et al*.Highly sensitive sensing of a magnetic field and temperature based on two open ring channels SPR-PCF. *Opt. Express.* 2022. **30**, No 21. P. 39055–39067. https://doi.org/10.1364/OE.470386.
7. Mamykin S.V., Gnilitskyi I.M., Dusheyko M.G. *et al*. Femtosecond laser nano-structuring for surface plasmon resonance-based detection of uranium. *Appl. Surf. Sci*. 2022. **576**. P. 151831. https://doi.org/10.1016/j.apsusc.2021.151831.
8. Yastrubchak O., Riney L., Powers W. *et al*. Band engineering of magnetic (Ga,Mn)As semiconductors by phosphorus doping. *IEEE Trans. Magn.* 2023. **59**, No 11. Art. No 1600106. https://doi.org/10.1109/TMAG.2023.3287730.
9. Gnilitskyi I., Mamykin S.V., Lanara C. *et al*. Laser nanostructuring for diffraction grating based surface plasmon-resonance sensors. *Nanomaterials*. 2021. **11**. P. 591. https://doi.org/10.3390/nano11030591.
10. Kushwaha M.S. Plasmons and magnetoplasmons in semiconductor heterostructures. *Surf. Sci. Rep*. 2001. **41**, No 1. P. 1–416. https://doi.org/10.1016/S0167-5729(00)00007-8.
11. Redko R.A., Milenin G.V., Milenin V.V. Radiative recombination in III-V semiconductors compounds and their surface morphology transformations due to treatments in weak magnetic fields. *J. Lumin*. 2019. **216**. P. 116678. https://doi.org/10.1016/j.jlumin.2019.116678.
12. Redko R., Milenin G., Milenin V. *et al*. Modification of GaN thin film on sapphire substrate optical properties under weak magnetic fields. *Mater. Res. Express*. 2018. **6**, No 3. P. 036413. https://doi.org/10.1088/2053-1591/aaf612.
13. Milenin G., Redko R. Transformation of structural defects in semiconductors under action of electromagnetic and magnetic fields causing resonant phenomena. *SPQEO*. 2019. **22**, No 1. P. 39–46. https://doi.org/10.15407/spqeo22.01.039.
14. Pakniyat S., Holmes A.M., Hanson G.W. *et al*. Non-reciprocal, robust surface plasmon polaritons on gyrotropic interface. *IEEE Trans. Antennas Propag.* 2020. **68**, No 5. P. 3718–3729. https://doi.org/10.1109/TAP.2020.2969725.
15. Belotelov V.I., Akimov I.A., Pohl M. *et al*. Enhanced magneto-optical effects in magneto-plasmonic crystals. *Nat. Nanotechnol.* 2011. **6**, No 6. P. 370–376. https://doi.org/10.1038/nnano.2011.54.
16. Simon M., Chauhan P. Anomalous absorption of *p*-polarised laser on metallic surface ingrained with noble-metal nanotubes in the presence of external magnetic field. *Opt. Quant. Electron*. 2023. **55**, No 9. P. 777. https://doi.org/10.1007/s11082-023-05088-x.
17. Saermark K., Lebech J., Johansen H.On the concept of cyclotron resonance in metals. *phys. status solidi* (*b*). 1977. **83**, No 1. P. 187–195. https://doi.org/10.1002/pssb.2220830121.
18. Suhl H. Cyclotron resonance revisited. *J. Phys. (France).* 1989. **50**, No 18. P. 2613–2627. https://doi.org/10.1051/jphys:0198900500180261300.
19. Malissa H., Wilamowski Z., Jantsch W. Cyclotron resonance revisited: the effect of carrier heating, *AIP Conf. Proc*. 2005. **772**, No 1. P. 1218–1219. https://doi.org/10.1063/1.1994551.
20. Lyaschuk Y., Indutnyi I., Myn'ko V. *et al*. Aluminum-based plasmonic photodetector for sensing applications. *Appl. Sci.* 2024. **14**, No 11. P. 4546. https://doi.org/10.3390/app14114546.
21. Schubert M., Kühne P., Darakchieva V. *et al*. Optical Hall effect – model description: tutorial. *J. Opt. Soc. Am. A.* 2016. **33**, No 8. P. 1553–1568. https://doi.org/10.1364/JOSAA.33.001553.

Authors' contributions

Redko R.A.: conceptualization, methodology, measurements, writing – review & editing.
Mamykin S.V.: investigation, validation, writing – review & editing, methodology.
Kondratenko O.S.: conceptualization, methodology, measurements, writing – original draft, writing – review & editing.
Savchuk Ye.M.: formal analysis, investigation.

Authors and CV

R.A. Redko, PhD in Physics and Mathematics (Solid-State Physics), Acting Scientific Secretary of ISP. Associate Professor at the State University of Information and Communication Technologies. The area of scientific interests is semiconductor physics and solid-state electronics.
https://orcid.org/0000-0001-9036-5852

S.V. Mamykin, PhD in Physics and Mathematics, Head of the Department. The area of scientific interests includes optics, optoelectronics, plasmonics, nanophotonics, sensorics and photoconverting devices.
E-mail: mamykin@isp.kiev.ua,
https:// orcid.org/0000-0002-9427-324X

O.S. Kondratenko, PhD in Physics and Mathematics, researcher at the Department of Polaritonic Optoelectronics and Technology of Nanostructures at the V. Lashkaryov Institute of Semiconductor Physics. The area of scientific interests includes optoelectronics, plasmonics, optics, nanophotonics, thin films. https://orcid.org/0000-0003-1948-4431, e-mail: kondratenko@isp.kiev.ua

Ye.M. Savchuk, MSc in Information Communication Networks, Junior Researcher. The area of scientific interests is semiconductor physics and plasmon-polariton photodetectors.
E-mail: liza.synelnyk@gmail.com,
https://orcid.org/0009-0009-7064-5051

Спричинений магнітним полем аномальний зсув піка плазмонного резонансу в плазмон-поляритонних фотодетекторах на основі алюмінію

Р.А. Редько, С.В. Мамикін, О.С. Кондратенко, Є.М. Савчук

Анотація. Досліджено вплив дії магнітного поля на залежності Ψ(λ) і Δ(λ) для плазмон-поляритонних фотодетекторів (ППФД) на основі алюмінію при різних значеннях магнітної індукції (100 і 300 мТл) і напрямках магнітного поля. Установлено, що дія магнітного поля приводить як до зсуву положення піка поверхневого плазмонного резонансу (ППР) досліджуваних структур, так і до зміни його інтенсивності. Виявлено, що в конфігурації $\vec{B} \perp \vec{n}$ ($\vec{B}$ та $\vec{E}$ колінеарні) відзначений ефект був найбільш вираженим. Додатково встановлено, що магнітний ефект чутливий до кута падіння, а саме, він посилюється при зменшенні кута падіння. Тому при найменшому куті в нашому експерименті (20°) він був найбільш вираженим. У роботі проаналізовано можливі фізичні механізми спостережуваних явищ. Отримані результати можуть відкрити нові можливості в конструюванні оптоелектронних датчиків магнітного поля або високошвидкісних оптичних модуляторів.

Ключові слова: поверхневий плазмонний резонанс, магнітне поле, плазмон-поляритонний фотодетектор.